multimedia

Simultaneous visualization of the translocation of protein kinase Cα–green fluorescent protein hybrids and intracellular calcium concentrations

Kasper ALMHOLT, Per O. G. ARKHAMMAR[1], Ole THASTRUP and Søren TULLIN

BioImage, Novo Nordisk A/S, 28 Mørkhøj Bygade, DK-2860 Søborg, Denmark

The α isoform of protein kinase C (PKCα) is a ubiquitous protein kinase, which, upon activation, translocates rapidly from the cytoplasm to the plasma membrane. To follow this translocation, PKCα was tagged with a highly fluorescent derivative of green fluorescent protein and stably expressed in baby hamster kidney cells overexpressing the muscarinic type 1 receptor. Addition of the agonist carbamylcholine triggered the onset of translocation within 1 s. Half-maximal and maximal translocation occurred after about 3 and 15 s respectively. Plasma membrane association of the fusion protein was transient and the protein returned to the cytoplasm within about 45 s. A high-resolution study showed an almost homogeneous cytoplasmic distribution of tagged PKCα in unstimulated cells and virtually complete translocation to the plasma membrane in response to the phorbol ester, PMA. Simultaneous visualization of intracellular calcium concentration ($[Ca^{2+}]_i$) and PKCα translocation in single cells showed a good correlation between these parameters at intermediate and high concentrations of agonist. At low agonist concentration, a small increase in $[Ca^{2+}]_i$ was observed, without detectable translocation of PKCα. In contrast, PMA induced translocation of PKCα without any increase in $[Ca^{2+}]_i$. Neither cytochalasin D nor colcemid influenced the distribution or calcium-dependent translocation of tagged PKCα, indicating that PKCα translocation may be independent of both actin filaments and microtubules. The time course of PKCα translocation is compatible with diffusion of the protein from its cytoplasmic localization to the plasma membrane.

INTRODUCTION

The advent of quin2 [1] and later fura2 [2] enabled direct monitoring of dynamic calcium changes at high temporal resolution in single cells. Likewise, it is evident that the appearance of green fluorescent protein (GFP) [3] will allow a similar dynamic and detailed characterization of the intracellular localization and movement of proteins, such as cytoskeletal components, phosphatases and kinases. In the case of a subgroup of kinases, movement seems to be a prerequisite to their phosphorylation of target substrates [4]. In such cases, translocation of the proteins can be regarded as diagnostic for their participation in signal transduction. In the present study, we describe for the first time simultaneous monitoring of intracellular calcium concentration ($[Ca^{2+}]_i$) and trafficking of a specific isoform of protein kinase C (PKC) [5,6].

The PKC serine/threonine protein kinase family includes at least 12 different isoforms. They have traditionally been divided into three groups based on amino acid sequence similarity and dependence upon phospholipid metabolites and calcium. The family comprises: the calcium-dependent conventional PKC (cPKC) isoforms α, βI, βII and γ, the calcium-independent novel PKC (nPKC) isoforms δ, ε, η and θ and the atypical PKC (aPKC) isoforms ι, λ and ζ, which are also calcium independent. In a recently described fourth subclass, the only member is the human μ isoform and its homologue in mice, protein kinase D [7,8]. In addition, cPKCs and nPKCs are regulated by 1,2-diacylglycerol (DAG) and phorbol esters, whereas aPKCs are not [8–10]. The activities of cPKCs, nPKCs and aPKCs are also regulated by phospholipids, in particular by phosphatidylserine (PS) to varying degrees [8].

The tissue distribution of the various PKC isoforms also varies notably. Of the cPKCs, the α isoform is found in most cell types, whereas the βI and βII isoforms are found preferentially in cells of neuronal and haematopoietic lineage [10]. Translocation of the majority of PKC isoforms from the cytoplasm to cellular membranes [9–11] is believed to precede and initiate their activation. For instance, it has been shown, using subcellular fractionation, that stimulation of the plasma membrane bound G_q-coupled muscarinic receptors induces rapid translocation of cPKCs [4,12] as well as fast phosphorylation of target substrates [4]. In this study we have activated the muscarinic receptor type 1 with the acetylcholine analogue carbamylcholine (carbachol), leading to activation of phospholipase Cβ, which generates DAG and Ins(1,4,5)P_3. In turn, Ins(1,4,5)P_3 promotes the release of calcium from intracellular stores [13]. Although the membrane lipids DAG and PS also play important roles in the activation of cPKCs, it has been shown that an elevated $[Ca^{2+}]_i$ alone induces cPKC translocation [14].

GFP offers a novel approach to study protein localization and trafficking in intact living cells [3]. Despite the relatively large size of GFP (238 amino acids), GFP-tagged proteins have been shown to be targeted properly in numerous cases [15]. Recently, GFP-tagged PKCγ has been demonstrated to transiently translocate in a calcium-dependent manner from a cytoplasmic to a plasma membrane localization in response to receptor stimu-

Abbreviations used: GFP, green fluorescent protein; $[Ca^{2+}]_i$, intracellular calcium concentration; PKC, protein kinase C; cPKC, nPKC and aPKC, conventional, novel and atypical PKC respectively; DAG, 1,2-diacylglycerol; PS, phosphatidylserine; carbachol, carbamylcholine; GFP^{LT}, GFP with F64L and S65T amino acid substitutions (using the single-letter symbols for amino acids); mPKC, murine PKC; BHK, baby hamster kidney; hM1, human muscarinic receptor type 1; FBS, fetal bovine serum; CCD, charged coupled device; AM, acetoxymethyl ester; Tg, thapsigargin; BAPTA, 1,2-bis-(*o*-aminophenoxy)ethane-*N*,*N*,*N*′,*N*′-tetra-acetic acid.

[1] To whom correspondence should be addressed (poga@novo.dk).

lation [16,17]. To investigate the trafficking of PKCα and its direct relationship to $[Ca^{2+}]_i$ in real time in intact living cells, we tagged the protein kinase with a highly fluorescent variant of GFP containing F64L and S65T amino acid substitutions (GFP^{LT}) [18]. We demonstrate here that trafficking of a GFP-tagged PKCα can be combined with simultaneous measurements of $[Ca^{2+}]_i$ using fura2. We conclude that receptor-mediated PKCα translocation is a very rapid phenomenon closely related to changes in $[Ca^{2+}]_i$.

MATERIALS AND METHODS

Hybrid cDNA construction

Hybrid cDNAs encoding N- and C-terminal fusions of murine PKCα (mPKCα) [19] to GFP^{LT} (mPKCα–GFP^{LT} and GFP^{LT}–mPKCα) were inserted into the multiple cloning site of the pZeoSV® (Invitrogen Corp., San Diego, CA, U.S.A.) mammalian expression vector. Briefly, cDNAs encoding mPKCα and GFP^{LT} were amplified by PCR using the following primers: 5′-mPKCα, TTGGACACAAGCTTTGGACACCCTCAGGATATGGCTGACGTTTACCCGGCCAACG; 3′-mPKCα, GTCATCTTCTCGAGTCTTTCAGGCGCGCCCTACTGCACTTTGCAAGATTGGGTGC; 5′-GFP^{LT}, TTGGACACAAGCTTTGGACACGGCGCGCCATGAGTAAAGGAGAAGAACTTTTC and 3′-GFP^{LT}, GTCATCTTCTCGAGTCTTACTCCTGAGGTTTGTATAGTTCATCCATGCCATGT.

*Hin*dIII/*Asc*I-digested mPKCα fragment and *Asc*I/*Xho*I-digested GFP^{LT} fragment were ligated with the *Hin*dIII/*Xho*I-digested vector, generating the mPKCα–GFP^{LT} fusion construct. Correspondingly, the GFP^{LT}–mPKCα construct was generated by ligating *Hin*dIII/*Bsu*36I-digested GFP^{LT} fragment and *Bsu*36I/*Xho*I-digested mPKCα fragment with the *Hin*dIII/*Xho*I-digested vector. To generate a similar construct which allowed the expression of GFP^{LT} alone, GFP^{LT} was inserted in the vector as a *Hin*dIII/*Xho*I fragment.

Cell cultures

The human muscarinic receptor type 1 (hM1) [20] was stably expressed in baby hamster kidney cells (BHK/hM1 cells; Novo Nordisk A/S, Bagsværd, Denmark) and maintained with the dihydrofolate reductase marker. These cells were transfected with the vectors containing hybrid cDNA for the mPKCα–GFP^{LT} or the GFP^{LT}–mPKCα fusion proteins or GFP^{LT} alone using the calcium phosphate precipitate method in Hepes-buffered saline [21]. Stable transfectants were selected using 1000 μg of Zeocin®/ml (Invitrogen) in growth medium [Dulbecco's modified Eagle's medium with 1000 mg of glucose/l and 10% (v/v) fetal bovine serum (FBS)] purchased from Life Technologies Inc., Gaithersburg, MD, U.S.A. The hM1 receptor and mPKCα–GFP^{LT} were maintained with 500 nM methotrexate and 500 μg of Zeocin®/ml respectively. For control purposes, the fusion proteins were stably expressed in BHK-21 cells (A.T.C.C., Rockville, MD, U.S.A.) without the hM1 receptor. Stably transfected cells will subsequently be referred to as, e.g. BHK/hM1,mPKCα–GFP^{LT} cells.

For fluorescence microscopy, cells were allowed to adhere to Lab-Tek chambered coverglasses (Nalge Nunc Int., Naperville, IL, U.S.A.) for at least 24 h and cultured to about 50% confluency. Before experiments, the cells were cultured overnight without selection pressure in HAM's F12 medium with glutamax (Life Technologies) and 0.3% (v/v) FBS. This medium has low autofluorescence, enabling fluorescence microscopy of cells straight from the incubator.

Subcellular fractionation

Stably transfected BHK/hM1 cells were separated into soluble and particulate fractions using an adaptation of a previously published method [22]. Immediately after treatment with buffer or PMA for 15 min at 37 °C, the cells were recovered from tissue-culture plates by washing with ice-cold Dulbecco's PBS (Life Technologies) followed by scraping and suspension in buffer A containing 20 mM Tris/HCl (pH 7.5), 0.25 M sucrose, 5 mM EDTA, 2 mM EGTA and freshly added 25 mM dithiothreitol, 1 mM PMSF and 200 μM Na_3VO_4. The cells were homogenized for 1 min in a Dounce homogenizer and centrifuged for 20 min at 100000 ***g***. Supernatants were collected as the soluble fractions. Pellets were resuspended in buffer A supplemented with 1% (v/v) Triton X-100 and incubated for 30 min. The extracts of the particulate fraction were centrifuged at 12000 ***g*** for 20 min, yielding the solubilized particulate fractions. The protein samples were concentrated using Centricon10 centrifuge concentrators (Amicon Inc., Beverly, MA, U.S.A.). All of the above steps were carried out at 4 °C unless otherwise stated.

Immunoblotting

Samples containing 10 μg of protein were added to SDS sample buffer [21] and run on precast 7.5% SDS/PAGE gels with a 4% stacking gel (Bio-Rad Laboratories, Hercules, CA, U.S.A.). The proteins were transferred to PH79 nitrocellulose membranes (Scleicher & Schuell GmbH., Dassel, Germany). Proteins were detected using standard techniques. Antibodies used were the primary polyclonal rabbit anti-PKCα antibody (Sigma P-4334), diluted 1:10000 and the secondary horseradish peroxidase-conjugated donkey anti-rabbit immunoglobulin (Amersham International plc., Amersham, Bucks., U.K.) diluted 1:5000. Immunoreactivity was detected by enhanced chemiluminescence (ECL) as described by the manufacturer (Amersham) and exposed on Biomax® MR film (Eastman Kodak Company, Rochester, NY, U.S.A.).

Fluorescence microscopy and computer-assisted imaging

Time-lapse recording of mPKCα–GFP^{LT} movement

BHK/hM1,mPKCα–GFP^{LT} cells were cultured in HAM's F12 medium as described above. The chambers were placed on a temperature-regulated microscope stage and kept at 37 °C. Fluorescence images were captured using an Axiovert 135M inverted light microscope (Carl Zeiss, Oberkochen, Germany) equipped with a Fluar 40×, numerical aperture 1.3 oil immersion objective (Zeiss) and a cooled (−40 °C) CH250 charged coupled device (CCD) camera (Photometrics Ltd., Tucson, AZ, U.S.A.) with a KAF1400 1340×1037 pixel CCD chip. The microscope was also equipped with a 470±20 nm excitation filter, a 505 nm dichroic mirror and a 515±15 nm emission filter (Delta Lys & Optik, Lyngby, Denmark). The excitation light source was a 100 W HBO arc lamp. The images obtained by time-lapse recording were then analysed using the IPLab Spectrum software package (Signal Analytics Corp., Vienna, VI, U.S.A.). The translocation of the fusion protein was measured by tracing two regions of interest corresponding to the brightest part of the perinuclear cytoplasm (covering roughly 20% of the cell area) and the peripheral 5 μm of the cell, i.e. the plasma membrane. The average fluorescence intensity of these regions, divided by the average fluorescence intensity of the entire cell, to correct for bleaching, was calculated for every image in the time-lapse series. Bleaching was in the range 2–15% for an image series, depending on exposure time and number of images. The temporal information thus acquired is expressed throughout as mean±S.D.

High-resolution imaging of mPKCα–GFP^{LT} distribution before and after PMA stimulation

High-resolution images of single BHK/mPKCα–GFP^{LT} cells were generated from three-dimensional data sets collected using the microscope set-up as described above. Optical sections were acquired through the entire cell at 0.25 μm focal intervals. Captured images had an effective pixel size of 0.164 μm × 0.164 μm. After acquisition, the data sets were corrected for bleaching and fluctuations in illumination intensity. The out-of-focus information in the images was then removed using iterative, constrained three-dimensional deconvolution (DeltaVision from Applied Precision Inc., Seattle, WA, U.S.A.) based on a theoretically calculated point-spread function.

Simultaneous measurement of mPKCα–GFP^{LT} movement and changes in $[Ca^{2+}]_i$

BHK/hM1,mPKCα–GFP^{LT} cells, cultured in HAM's F12 medium as described above, were loaded with 0.5 μM fura2 acetoxymethyl ester (fura2/AM) (Molecular Probes Inc., Eugene, OR, U.S.A.) in Ca^{2+}-Hepes buffer, pH 7.4, containing 10 mM Hepes, 140 mM NaCl, 5 mM KCl, 5.5 mM D-glucose, 1 mM $MgSO_4$ and 1 mM $CaCl_2$ for 30 min at 37 °C. The fura2-loaded cells were placed on the temperature-regulated stage of a Diaphot300 microscope (Nikon Corp., Tokyo, Japan) equipped with a second generation CXTI intensified video camera (Photonic Science Ltd., East Sussex, U.K.). The cells were illuminated with a Polychrome I monochromator (T.I.L.L. Photonics GmbH., Planegg, Germany). In the light path was a 490 nm dichroic mirror and a 515 ± 15 nm emission filter. To reduce background fluorescence, a 415 ± 75 nm excitation filter was included. GFP^{LT} fluorescence was monitored by exciting at 470 nm, whereas fura2 was excited with alternating 340 and 380 nm light.

The fluorescence ratio between 340 and 380 nm images were converted into $[Ca^{2+}]_i$ by using the equation $[Ca^{2+}]_i = K_D[(R-R_{min})/(R_{max}-R)]\beta$ [2], where the dissociation constant K_D is 224 nM and R is the 340/380 fluorescence ratio at each image pixel corrected for background. The internal constants for the system were measured using fura2 pentapotassium salt (Molecular Probes) in solution and found to be $R_{min} = 0.15$, $R_{max} = 6.16$ and $\beta = 6.27$. The GFP^{LT} fusion protein gave a small contribution to background fluorescence at 380 nm but none at 340 nm. Fura2 did not contaminate the signal at 470 nm. However, with the temporal resolution of these experiments, there was a significant spill-over from one frame to the next due to relaxation lag of the image intensifier. The implication is that basal calcium values were overestimated and extreme values underestimated. While the effect on the GFP^{LT} signal was corrected by dividing by the average fluorescence intensity of the entire cell, we decided to sacrifice precision of the calculated $[Ca^{2+}]_i$ values to obtain maximal temporal resolution. Importantly, the dynamics of $[Ca^{2+}]_i$ and mPKCα–GFP^{LT} translocation remained undisturbed. The average cytoplasmic $[Ca^{2+}]_i$ was calculated within a region of interest corresponding to the non-nuclear cytoplasm in the cell image, whereas mPKCα–GFP^{LT} trafficking was followed using the method described in the 'Time-lapse recording of mPKCα–GFP^{LT} movement' section.

The integrated calcium response or mPKCα–GFP^{LT} translocation over time was computed in each individual cell as the area between the observed data and a hypothetical baseline created by interpolating the data acquired before agonist addition and after the return of calcium or the fusion protein to basal level. The qualitatively different responses seen with 10 μM ionomycin were not included in this calculation.

RESULTS

GFP^{LT}-tagged mPKCα translocated in parallel with endogenous PKCα

To monitor PKCα trafficking in real time in living cells, either mPKCα–GFP^{LT} or GFP^{LT}–mPKCα was stably expressed in BHK/hM1 cells. To compare the translocation of the two fusion proteins with that of the endogenous PKCα in response to various agonists, we performed subcellular fractionation on BHK/hM1,mPKCα–GFP^{LT} cells (Figure 1A), BHK/hM1, GFP^{LT}–mPKCα cells (Figure 1B) and on control BHK/hM1,GFP^{LT} cells (Figure 1C). The cells were stimulated with buffer or 100 nM PMA, separated into soluble and particulate fractions and characterized by Western blot analysis using polyclonal antibodies directed against the C-terminus of PKCα. This experiment indicated that both fusion proteins had the expected molecular mass (Figures 1A and 1B). The two fusion proteins and the endogenous PKCα translocated in parallel from the soluble to the particulate fraction after stimulation with PMA for 15 min (Figure 1). Owing to possible differential recognition of endogenous hamster PKCα and overexpressed mouse fusion proteins by the antibody employed, their expression levels might not be directly comparable. Note that the expression level of mPKCα–GFP^{LT} might be underestimated, since the C-terminal PKCα epitope recognized by the antibody is masked by the fusion to GFP^{LT}. Most experiments described below have been conducted with both fusion proteins, although for brevity we have chosen to concentrate on the results obtained with mPKCα–GFP^{LT}.

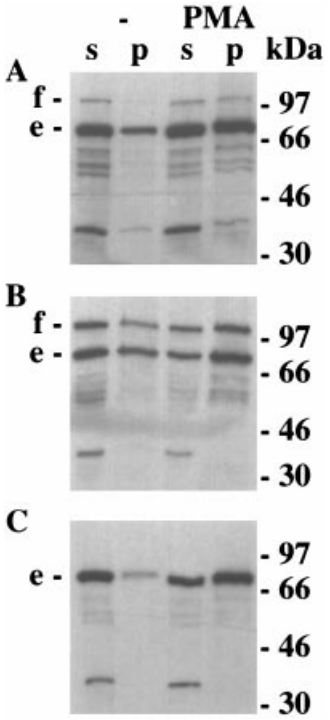

Figure 1 Western blots

BHK/hM1 cells expressing either mPKCα–GFP^{LT} (**A**), GFP^{LT}–mPKCα (**B**) or GFP^{LT} alone (**C**) were stimulated for 15 min with buffer (—) or 100 nM PMA. Total lysates were subjected to subcellular fractionation yielding soluble (s) and particulate (p) fractions. The two fusion proteins (f) had the expected molecular mass of 104 kDa. The endogenous PKCα (e) had a molecular mass of 77 kDa.

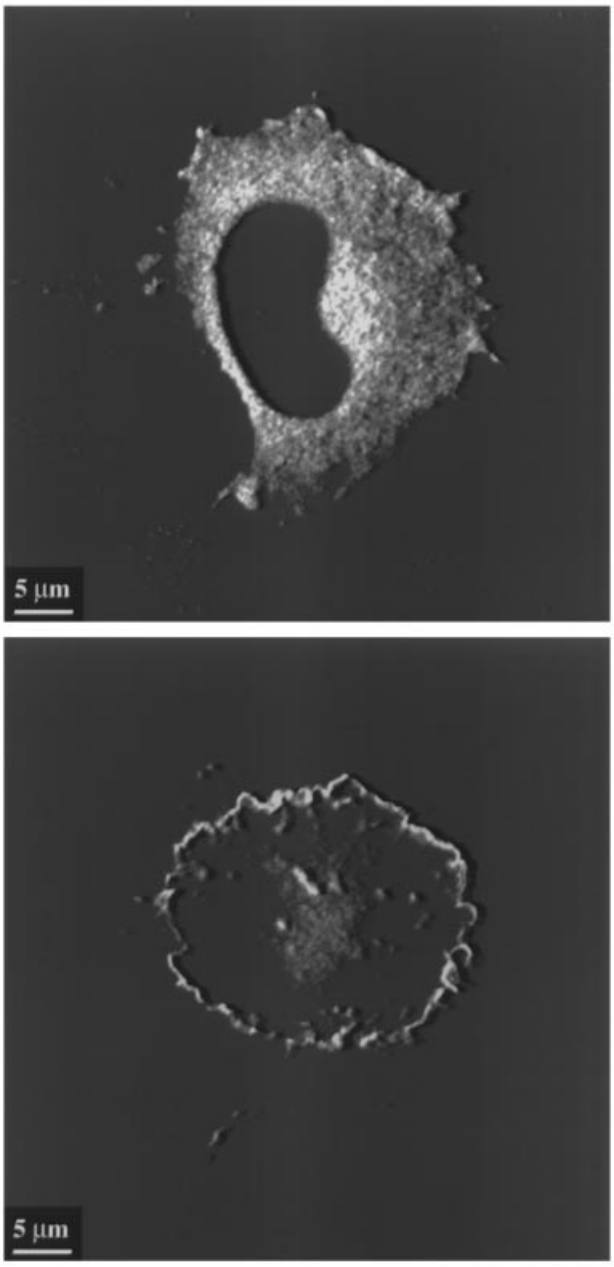

Figure 2 High-resolution imaging of mPKCα–GFP^{LT} localization

The subcellular localization of mPKCα–GFP^{LT} was studied before (top) and 15 min after (bottom) stimulation with 100 nM PMA by using digitally deconvolved Z-series of wide-field images. From the deconvolved images, five single slices were merged into 1 μm thick reconstructed slices from the same BHK/hM1,mPKCα–GFP^{LT} cell before and after stimulation and are shown here as two-dimensional representations, the slices being 1.5 μm above the substratum. The images shown are representative for results from three separate experiments.

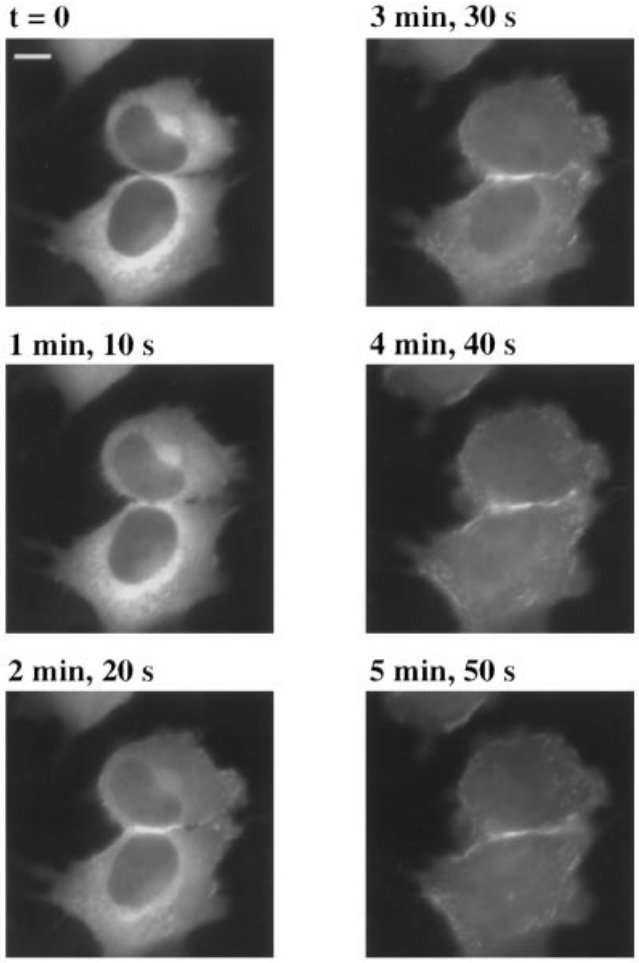

Figure 3 Time-lapse analysis of PMA-induced mPKCα–GFP^{LT} translocation

mPKCα–GFP^{LT} translocation in response to 100 nM PMA given immediately after $t = 0$ was analysed by time-lapse fluorescence microscopy. The micrograph series shown is representative of five independent observations. Scale bar = 10 μm. Time-lapse movies are available at URL: http://www.BiochemJ.org/bj/337/bj3370211add.htm

Response to PMA

The subcellular distribution of mPKCα–GFP^{LT} was studied in high spatial resolution using digitally deconvolved Z-series of wide-field images. Two-dimensional reconstructions, 1 μm thick (based on five 0.25 μm slices), are shown (Figure 2). In unstimulated cells, the fusion protein was distributed fairly homogeneously throughout the cytoplasm, with a somewhat higher concentration in the perinuclear region (Figure 2A). Stimulation with 100 nM PMA caused the cells to round up and the fusion protein to translocate evenly to all parts of the plasma membrane, with a concomitant depletion of the cytoplasm (Figure 2B). The remaining central fluorescence is likely to be associated with the basal plasma membrane since the slice was taken close to the substratum. We cannot, however, based on the present experiments, exclude that a fraction of this fluorescence actually is cytoplasmic.

Wide-field fluorescence micrograph time-lapse series showed that 100 nM PMA induced complete and permanent (cells were followed up to 2 h) translocation of mPKCα–GFP^{LT} within 5 min (Figure 3). Bear in mind that mPKCα–GFP^{LT}, localized to the upper region of the plasma membrane, erroneously gives the impression of fusion protein remaining in the cytoplasm. It should be noted that the reverse GFP^{LT}–mPKCα fusion protein behaved in a similar way in response to PMA ($n = 2$, results not shown).

Response to carbachol

As shown in Figure 4, 100 μM carbachol caused a fast and transient translocation of mPKCα–GFP^{LT} to the plasma mem-

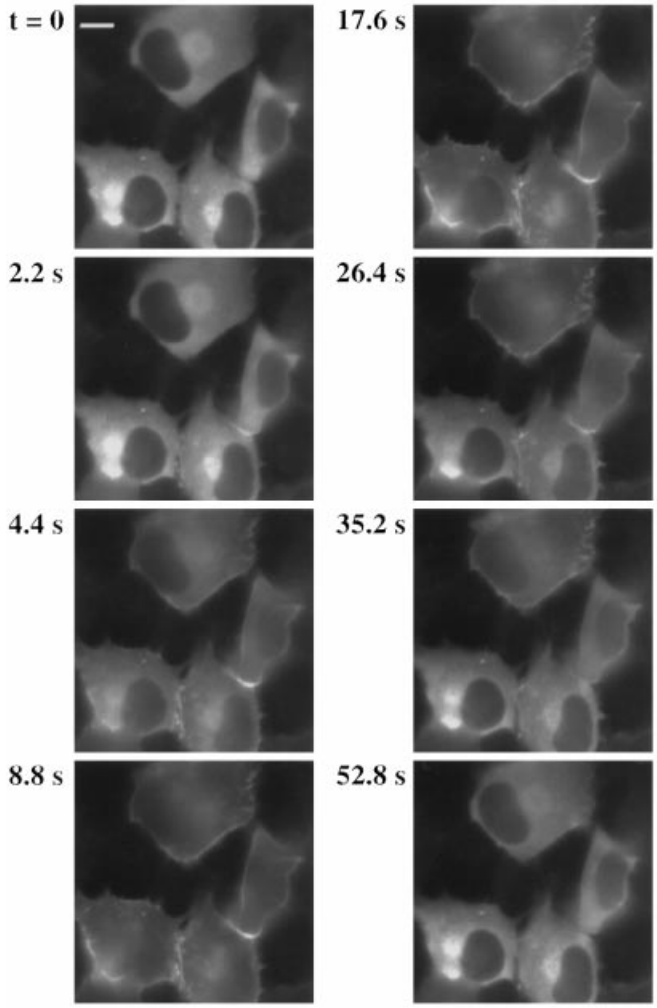

Figure 4 Time-lapse analysis of carbachol-induced mPKCα–GFP^{LT} translocation

mPKCα–GFP^{LT} translocation in response to 100 μM carbachol given immediately after $t = 0$ was analysed by time-lapse fluorescence microscopy. The micrograph series shown is representative of 30 independent observations. Scale bar = 10 μm. Time-lapse movies are available at URL: http://www.BiochemJ.org/bj/337/bj3370211add.htm

brane. The temporal profile of the response was characterized as described. From 12 single cells in four independent experiments the following temporal profile was observed. The fusion protein was half-maximally translocated to the plasma membrane after 2.9 ± 0.4 s. Maximal translocation was observed after 14.7 ± 3.4 s and the fusion protein returned to an even distribution throughout the cytoplasm after 46 ± 6.1 s. This distribution was indistinguishable from the distribution observed before carbachol stimulation (Figure 4).

The reverse GFP^{LT}–mPKCα fusion protein behaved in a similar way in response to carbachol ($n = 7$, results not shown). Experiments conducted with BHK-21 cells stably expressing either of the fusion proteins, but without the coexpressed hM1 receptor, showed no PKCα translocation in response to high concentrations of carbachol ($n = 4$, results not shown). However, a translocation similar to that presented in Figure 3, was observed in response to 100 nM PMA ($n = 4$, results not shown). It should also be mentioned that addition of buffer did not induce fusion protein translocation ($n = 2$, results not shown) and that GFP^{LT} alone, expressed in BHK/hM1 cells, was distributed evenly throughout the cells and neither 50 nM PMA ($n = 2$) nor 50 μM carbachol ($n = 3$) had any effect on its diffuse distribution pattern (results not shown).

Monitoring of PKCα trafficking and $[Ca^{2+}]_i$

The importance of $[Ca^{2+}]_i$ for the translocation of PKCα was investigated using several approaches. BHK/hM1,mPKCα–GFP^{LT} cells were pretreated for 5 min with 1 μM thapsigargin (Tg) [23]. This treatment inhibited the translocation of mPKCα–GFP^{LT} in response to 100 μM carbachol by $97.5 \pm 4\%$ ($n = 8$), while the accompanying change in $[Ca^{2+}]_i$ was inhibited by $99.7 \pm 0.2\%$ ($n = 5$, separate experiments). Similarly, the cells were loaded with 10 μM 1,2-bis-(*o*-aminophenoxy)ethane-*N*,*N*,*N*′,*N*′-tetra-acetic acid (BAPTA)/AM, a cell permeant non-fluorescent calcium chelator. This treatment inhibited the translocation in response to 100 μM carbachol by $62.5 \pm 6\%$ ($n = 7$), whereas the accompanying change in $[Ca^{2+}]_i$ was inhibited by $66.8 \pm 4\%$ ($n = 6$, separate experiments). However, neither Tg treatment ($n = 3$) nor BAPTA/AM loading ($n = 4$) changed the mPKCα–GFP^{LT} translocation in response to 100 nM PMA. Under these circumstances no change in $[Ca^{2+}]_i$ was observed (Tg: $n = 3$, BAPTA/AM: $n = 6$, separate experiments).

To investigate the temporal relationship of changes in $[Ca^{2+}]_i$ and PKCα translocation with high time resolution, we loaded BHK/hM1,mPKCα–GFP^{LT} cells with 0.5 μM fura2/AM, a cell permeant fluorescent calcium probe. $[Ca^{2+}]_i$ and mPKCα–GFP^{LT} were monitored simultaneously by exciting the cells at 340, 380 and 470 nm in rapid succession. Such sets of three images were acquired consecutively at 400 ms intervals. The $[Ca^{2+}]_i$ was computed based on the images acquired with excitation at 340 and 380 nm, whereas trafficking of mPKCα–GFP^{LT} was followed in the images acquired with excitation at 470 nm (Figure 5).

The translocation of mPKCα–GFP^{LT} in response to carbachol observed under these conditions had a similar temporal profile (Table 1) as that described in the previous section. With the temporal resolution of these experiments we were unable to separate the initial calcium rise after carbachol or ionomycin stimulation from the onset of PKCα translocation to the plasma membrane. Both responses were initiated within the same 400 ms interval. However, it is evident from Table 1 and Figure 5 that, in the case of both carbachol and ionomycin, the calcium response preceded the translocation of PKCα. There was a tendency to a slower PKCα translocation in response to carbachol in these experiments compared with the cells not loaded with fura2. In particular, half-maximal translocation was reached after about 8 s (Table 1) in fura2-loaded cells stimulated with 100 μM carbachol, whereas the time required in cells not loaded with the indicator was 2.9 ± 0.4 s.

The degree of PKCα translocation in response to carbachol correlated with the increase in $[Ca^{2+}]_i$ (Figure 5A–5C). The most pronounced increase in $[Ca^{2+}]_i$ was observed with 100 μM carbachol, coincident with the highest degree of PKCα translocation, whereas 1 μM carbachol gave a reproducible, although small, increase in $[Ca^{2+}]_i$, but no detectable PKCα translocation. At 10 μM carbachol the increase in $[Ca^{2+}]_i$ and the degree of PKCα translocation were intermediate. For each cell, the integrated mPKCα–GFP^{LT} translocation is plotted directly against the integrated calcium response in Figure 5(D), regardless of carbachol dose. Similarly, stimulation with ionomycin also showed correlation between changes in $[Ca^{2+}]_i$ and the degree of PKCα translocation (Figure 5E–5G): 10 μM ionomycin gave a sustained increase in $[Ca^{2+}]_i$, coincident with a sustained trans-

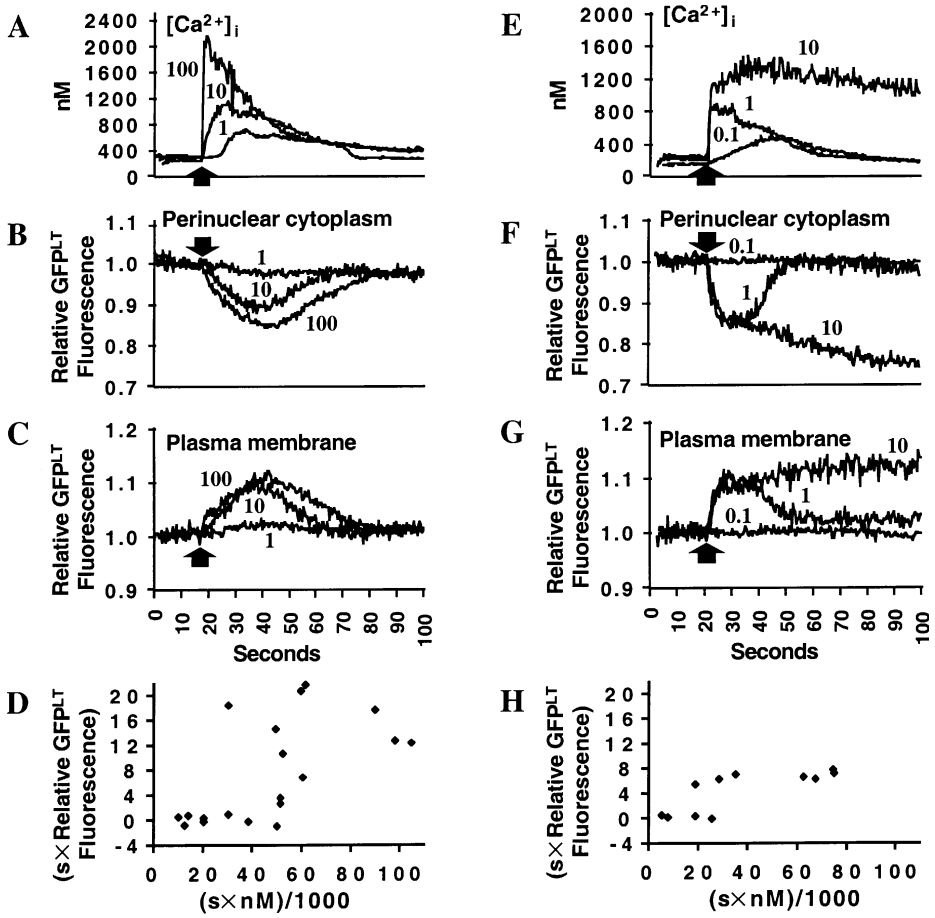

Figure 5 Simultaneous monitoring of mPKCα–GFP^{LT} and $[Ca^{2+}]_i$

Fura2-loaded BHK/hM1,mPKCα–GFP^{LT} cells were stimulated with three different concentrations of carbachol (**A**–**D**) or ionomycin (**E**–**H**). $[Ca^{2+}]_i$ (**A** and **E**) was monitored simultaneously with movement of mPKCα–GFP^{LT}, as seen by the change in relative fluorescence intensity (arbitrarily set to 1 at the beginning of each experiment) of the perinuclear cytoplasm (**B** and **F**) and the plasma membrane (**C** and **G**). As indicated in the graphs, cells were stimulated with either 1 μM, 10 μM or 100 μM carbachol or with 0.1 μM, 1 μM or 10 μM ionomycin. Arrows indicate the addition of agonist. The integrated responses over time were computed as described in the Materials and methods section on the basis of graphs similar to those shown in (**A** and **B**) and (**E** and **F**). The integrated mPKCα–GFP^{LT} translocation away from the cytoplasm is plotted directly against the corresponding integrated calcium responses to evaluate the correlation of these parameters independent of carbachol or ionomycin dose. Such results from 5–8 cells from three independent experiments for each carbachol concentration are shown in (**D**) while results from 4–7 cells from two independent experiments for each ionomycin concentration are shown in (**H**). Results from addition of 10 μM ionomycin have been omitted from (**H**) as they are qualitatively different. Integrated calcium and translocation measurements are highly correlated with Rank correlations of 0.65, $P = 0.003$ (**D**) and 0.79, $P = 0.004$ (**H**) respectively.

Table 1 Time from initiation of a response to half-maximal $[Ca^{2+}]_i$ and mPKCα–GFP^{LT} translocation ($t_{1/2\ max}$)

The results were extracted from curves such as those shown in Figures 5(A)–5(C) and 5(E)–5(G). All $t_{1/2\ max}$ values are given as means ± S.D. and are based on 4–8 cells from 2–3 independent experiments for each agonist concentration.

	$t_{1/2\,max}$	
Agonist (μM)	$[Ca^{2+}]_i$	mPKCα–GFP^{LT}
Carbachol		
100	0.8 ± 0.5	8.0 ± 1.0
10	1.2 ± 0.7	5.2 ± 1.7
1	11.5 ± 6.3	–
Ionomycin		
10	1.0 ± 0.3	4.6 ± 2.8
1	1.3 ± 0.1	4.2 ± 0.4
0.1	8.7 ± 2.7	–

location of PKCα to the plasma membrane; 1 μM ionomycin gave a substantial calcium transient and a transient PKCα translocation; and 0.1 μM ionomycin gave a significant, although small, increase in $[Ca^{2+}]_i$, but no detectable PKCα translocation. For each cell, the integrated mPKCα–GFP^{LT} translocation is plotted directly against the integrated calcium response in Figure 5(H) for ionomycin doses 0.1 and 1 μM. Rank correlation of the results in Figures 5(D) and 5(H) indicated a high probability for a positive correlation between PKCα translocation and $[Ca^{2+}]_i$ ($P < 0.01$) in response to carbachol or ionomycin. In contrast, the translocation of mPKCα–GFP^{LT} in response to 100 nM PMA observed under these conditions was not accompanied by any change in $[Ca^{2+}]_i$ (Figure 6).

Possible influence of the cytoskeleton

The cells rounded up in response to 10 μM ionomycin. The onset of this morphological change was about 1 min after addition of

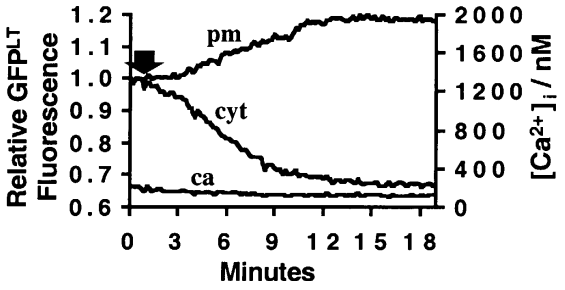

Figure 6 PMA does not elicit a calcium response

Fura2-loaded BHK/hM1,mPKCα–GFP^{LT} cells were stimulated with 100 nM PMA ($n = 3$) as indicated by the arrow. [Ca^{2+}]$_i$ (ca) was monitored simultaneously with movement of mPKCα–GFP^{LT}, as seen by the change in relative fluorescence intensity (arbitrarily set to 1 at the beginning of each experiment) of the perinuclear cytoplasm (cyt) and the plasma membrane (pm). The slow permanent translocation of mPKCα–GFP^{LT} to the plasma membrane was not accompanied by any change in [Ca^{2+}]$_i$.

agonist, i.e. long after fusion protein translocation was complete. No significant morphological changes were observed with carbachol or the lower concentrations of ionomycin.

To assess whether the cytoskeleton influences or controls the redistribution of PKCα we stimulated cells with 10 μM ionomycin, after 20 min preincubation with 1 μg/ml colcemid ($n = 4$), to depolymerize microtubules, or with 1 μM cytochalasin D ($n = 6$) to block the formation of F-actin. Both drugs caused some rounding of the cells at the concentrations used, but did not by themselves cause any redistribution of mPKCα–GFP^{LT} beyond confinement within the altered shape of the cells. The subsequent addition of ionomycin caused a permanent redistribution of fusion protein, much like the response seen in cells not treated with anticytoskeletal drugs.

DISCUSSION

The aim of the present study was to follow the trafficking of PKCα in real time in intact living cells with high spatial resolution. In addition, we wanted to correlate this process with intracellular calcium changes. To achieve this, we generated N- and C-terminal fusion proteins of mPKCα to a highly fluorescent variant of GFP. The following observations suggest that both fusion proteins behave like the endogenous kinase with regard to localization and trafficking. We found GFP^{LT}–mPKCα and mPKCα–GFP^{LT} in the same subcellular fraction as the endogenous kinase, before and after stimulation with phorbol ester. The partition of PKCα between soluble and particulate fractions agrees with previous studies using this fractionation method [22]. Furthermore, the intracellular localization of fusion protein in BHK/hM1,mPKCα–GFP^{LT} cells, before and after stimulation with PMA or carbachol, was very similar to the localization of endogenous PKCα in smooth muscle cells before and after stimulation with phenylephrine respectively, as visualized by immunocytochemistry [24]. Thus, it is reasonable to presume that PKCα trafficking can be studied in an isoform-specific manner using either of the described fusion proteins.

The time course of PMA-induced translocation described herein is comparable with results from a previous study in smooth muscle cells [25] where a fluorescently tagged phorbol ester, used both to track and activate PKCs, caused their translocation after about 2 min. It should be stressed that treatment of cells with Tg or loading with the calcium chelator BAPTA did not noticeably affect the fusion protein translocation in response to PMA, nor did PMA in itself cause a change in [Ca^{2+}]$_i$. Thus the PMA-induced translocation seems to be independent of an increase in [Ca^{2+}]$_i$. According to a previous study, PKCα translocated to the endoplasmic reticulum as well as to the plasma membrane after PMA stimulation [11]. The reason for this discrepancy is not clear, but our results are strengthened by the fact that individual cells were followed dynamically during the entire process of translocation. Although the translocation of fusion protein in response to PMA is accompanied by a rounding up of cells, we have no reason to suspect that this major morphological change has any influence on the partition of fusion protein between the cytoplasm and plasma membrane, since a very similar redistribution was observed in response to carbachol without any morphological changes. Furthermore, a previous study [25] has elegantly shown that PMA-inducible PKC translocation clearly precedes cell contraction in smooth muscle cells, although they both occur within about 2 min.

The temporal profile of carbachol-induced translocation reported here extends the conclusions of previous studies, based on subcellular fractionation, where the earliest time points are 15 s. These reports show rapid and transient translocation from a soluble to a particulate fraction of PKCα [4,26] and of PKCs in general [12]. We followed PKCα translocation with a higher temporal resolution and found that the initial calcium rise preceded the onset of translocation by less than 400 ms. The calcium increase in these cells was very steep, reaching half maximum after about 1 s in response to high or intermediate doses of carbachol or ionomycin, whereas PKCα translocation under the same conditions was half-maximal after 4–8 s. The fusion protein returned to the same localization as before stimulation within 1 min. Carbachol did not induce PKCα translocation in cells pretreated with Tg and translocation was attenuated in cells loaded with the calcium chelator BAPTA. This suggests that an elevated [Ca^{2+}]$_i$ is necessary for receptor-induced translocation in our system. Futhermore, these observations imply that an increased DAG concentration alone was insufficient for PKCα translocation. We also observed that ionomycin induced either a transient or permanent PKCα translocation. Taken together these observations may indicate, as reported earlier [14], that an elevated [Ca^{2+}]$_i$ is sufficient for PKCα translocation, without a concomitant increase in the concentration of DAG or PS. It has previously been proposed that there is a threshold value of [Ca^{2+}]$_i$ for translocation of PKCα [24]. Simultaneous monitoring of mPKCα-GFP^{LT} and [Ca^{2+}]$_i$ supports this notion, since small increases in [Ca^{2+}]$_i$ did not produce any detectable PKCα translocation. However, due to the imprecision of the calculated [Ca^{2+}]$_i$ values, we are reluctant to give an absolute value for this threshold.

With regard to the molecular mechanism behind PKC translocation, it is tempting to implicate the cytoskeleton, based on previous work where an association between PKC isoforms and cytoskeletal components was reported [11,27,28]. However, in parallel with a previous study on PKCγ translocation [16], our observation that disturbance of microtubules or actin filaments did not influence the distribution or calcium-dependent translocation of fusion protein does not point to a direct involvement of the cytoskeleton in the mechanism of PKCα translocation. In fact, although the translocation reported here is very rapid, it does not necessarily require an active transport process. We can estimate a diffusion coefficient for the 104 kDa fusion protein in the cytoplasmic matrix under the assumption that Stokes' Law, describing the movement of a sphere with a constant velocity through a viscous liquid, can be applied to globular proteins. With a diffusion coefficient of GFP in water of 8.7×10^{-7} cm^2/s

[29,30], and a roughly 5-fold higher viscosity for translational diffusion in the cytoplasm compared with water [30,31], we calculate a diffusion coefficient for mPKCα–GFP^{LT} in cytoplasm of 1.1×10^{-7} cm^2/s. The implication of this value is that cytoplasmic fusion protein on average travels about 10 μm by diffusion alone within 4.5 s. This timing is compatible with our observation of maximal and half-maximal translocation of mPKCα–GFP^{LT} after 14.7 ± 3.4 s and 2.9 ± 0.4 s respectively.

The present observations are compatible with a model for PKC translocation previously proposed by Mochly-Rosen [32]. In that model there is a weak interaction in unstimulated cells between PKC and an anchoring component in the target compartment. When the signal is present, it increases the affinity of the kinase for the target molecule, which shifts the equilibrium of PKC to favour the bound form. Applied to the present results, the diffusional equilibrium of PKCα would shift towards the plasma membrane bound form upon signal generation.

In conclusion we demonstrate that the trafficking of a GFP-tagged specific isoform of PKC can be followed simultaneously with measurements of $[Ca^{2+}]_i$ in single living cells. Our results suggest that a definite increase in $[Ca^{2+}]_i$ is necessary for receptor-mediated PKCα translocation. The present findings give no support for a direct role for the cytoskeleton in PKCα translocation. Indeed, the timing of this event is such that it may be explained by mere diffusion of the protein to the plasma membrane from its apparent cytoplasmic localization.

We thank Dr. S. P. Bjørn, Novo Nordisk A/S for developing a mutagenized cDNA clone for the highly fluorescent GFP^{LT} derivative, Dr. S. Rose-John, Johannes Gutenberg-Universität, Mainz, Germany for providing us with his cDNA clone of murine PKCα, and O. Skyggebjerg, Novo Nordisk A/S for customizing three-wavelength imaging for use in this study.

REFERENCES

1 Tsien, R. Y., Pozzan, T. and Rink, T. J. (1982) J. Cell Biol. **94**, 325–334
2 Grynkiewicz, G., Poenie, M. and Tsien, R. Y. (1985) J. Biol. Chem. **260**, 3440–3450
3 Chalfie, M., Tu, Y., Euskirchen, G., Ward, W. W. and Prasher, D. C. (1994) Science **263**, 802–805
4 Trilivas, I., McDonough, P. M. and Brown, J. H. (1991) J. Biol. Chem. **266**, 8431–8438
5 Takai, Y., Kishimoto, A., Inoue, M. and Nishizuka, Y. (1977) J. Biol. Chem. **252**, 7603–7609
6 Inoue, M., Kishimoto, A., Takai, Y. and Nishizuka, Y. (1977) J. Biol. Chem. **252**, 7610–7616
7 Johannes, F.-J., Prestle, J., Eis, S., Oberhagemann, P. and Pfizenmaier, K. (1994) J. Biol. Chem. **269**, 6140–6148
8 Newton, A. C. (1997) Curr. Opin. Cell Biol. **9**, 161–167
9 Dekker, L. V. and Parker, P. J. (1994) Trends Biochem. Sci. **19**, 73–77
10 Ohno, S. and Suzuki, K. (1995) in The Protein Kinase Facts Book: Protein-Serine Kinases (Hardie, G. and Hanks, S., eds.), pp. 80–88, Academic Press Ltd., London, UK
11 Goodnight, J., Mischak, H., Kolch, W. and Mushinski, J. F. (1995) J. Biol. Chem. **270**, 9991–10001
12 Messing, R. O., Stevens, A. M., Kiyasu, E. and Sneade, A. B. (1989) J. Neurosci. **9**, 507–512
13 Clapham, D. E. (1995) Cell **80**, 259–268
14 Trilivas, I. and Brown, J. H. (1989) J. Biol. Chem. **264**, 3102–3107
15 Gerdes, H.-H. and Kaether, C. (1996) FEBS Lett. **389**, 44–47
16 Sakai, N., Sasaki, K., Ikegaki, N., Shirai, Y., Ono, Y. and Saito, N. (1997) J. Cell Biol. **139**, 1465–1476
17 Oancea, E., Teruel, M. N., Quest, A. F. and Meyer, T. (1998) J. Cell Biol. **140**, 485–498
18 Thastrup, O., Tullin, S., Poulsen, L. K. and Bjørn, S. P. (1997) Novel variants of green fluorescent protein, GFP, International Application published under the Patent Cooperation Treaty (PCT). International Publication Number WO97/11094
19 Rose-John, S., Dietrich, A. and Marks, F. (1988) Gene **74**, 465–471
20 Peralta, E. G., Ashkenazi, A., Winslow, J. W., Smith, D. H., Ramachandran, J. and Capon, D. J. (1987) EMBO J. **6**, 3923–3929
21 Sambrook, J., Fritsch, E.-F. and Maniatis, T. (1989) Molecular Cloning: A Laboratory Manual, 2nd Edn., Cold Spring Harbor Laboratory, Cold Spring Harbor, NY
22 Hong, D.-h., Huan, J., Ou, B.-r., Yeh, J.-y., Saido, T. C., Cheeke, P. R. and Forsberg, N. E. (1995) Biochim. Biophys. Acta **1267**, 45–54
23 Thastrup, O., Cullen, P. J., Drøbak, B. K., Hanley, M. R. and Dawson, A. P. (1990) Proc. Natl. Acad. Sci. U.S.A. **87**, 2466–2470
24 Khalil, R. A., Lajoie, C. and Morgan, K. G. (1994) Am. J. Physiol. **266**, C1544–C1551
25 Khalil, R. A. and Morgan, K. G. (1991) Circ. Res. **69**, 1626–1631
26 Ha, K.-S. and Exton, J. H. (1993) J. Biol. Chem. **268**, 10534–10539
27 Jaken, S., Leach, K. and Klauck, T. (1989) J. Cell Biol. **109**, 697–704
28 Kiley, S. C. and Jaken, S. (1990) Mol. Endocrinol. **4**, 59–68
29 Terry, B. R., Matthews, E. K. and Haseloff, J. (1995) Biochem. Biophys. Res. Commun. **217**, 21–27
30 Swaminathan, R., Hoang, C. P. and Verkman, A. S. (1997) Biophys. J. **72**, 1900–1907
31 Luby-Phelps, K., Taylor, D. L. and Lanni, F. (1986) J. Cell Biol. **102**, 2015–2022
32 Mochly-Rosen, D. (1995) Science **268**, 247–251

Received 30 April 1998/22 September 1998; accepted 29 October 1998